Exploring the Hidden Constraints that Control the Self-Assembly of Nanomolecular Inorganic Clusters

School of Chemistry, University of Glasgow, University Avenue, Glasgow, G12 8QQ, UK.

Leroy Cronin*

Received, September 24, 2021; Accepted, October 18, 2021; Published, November 30, 2021

The mechanism that controls the self-assembly of complex polyoxometalate inorganic clusters in solution is a challenge because the clusters can contain anywhere from 6 to 368 metal ions in a single molecule and are commonly assembled under 'one-pot' reaction conditions. Furthermore, harnessing the 'self-assembly' processes allows synthesis on a length-scale and with a degree of complexity which is not easily accessed by more traditional 'step-wise' synthesis routes. This class of molecules are important as they can be thought of as 'molecular metal oxides' and rival the size of proteins yet are based upon simple MO_x units (where M is Mo, W, V and sometimes Nb and x can be 4, 5, 6 or 7). Here we review the structures of the molybdenum-based clusters and then show how it is possible to not only control the architectures but explore the mechanism of formation invoking mechanisms that are normally found in biological systems. We describe how a simple inorganic salt can spontaneously form 'information-rich', autocatalytic sets of replicating inorganic molecules that work via molecular recognition based on the $[PMo_{12}O_{40}]^{3-}$, $\{PMo_{12}\}$ Keggin ion, and $[Mo_{36}O_{112}(H_2O)_{16}]^{8-}$, $\{Mo_{36}\}$ cluster. These small clusters are involved in an autocatalytic network, where the assembly of gigantic molybdenum blue wheels $[Mo_{154}O_{462}H_{14}(H_2O)_{70}]^{14-}$ $\{Mo_{154}\}$, $[Mo_{132}O_{372}(H_2O)_{72}(CH_3CO_2)_{30}]^{42-}$, $\{Mo_{132}\}$ ball containing 154 and 132 molybdenum clusters are templated by the smaller clusters which are themselves able to catalyze their own formation. Finally, We introduce assembly theory and show how assembly theory can be used to describe the constraints that need to be present to facilitate the assembly of the large clusters and explain how information theoretic arguments might be useful for designing highly functional and unsymmetrical inorganic molecules.

1. Introduction

Polyoxometalates (POMs) are discrete inorganic metal oxide clusters. The elements most commonly occurring are transition metals in Group V (V, Nb, and Ta) or group VI (Mo and W).[1] The molecules may be comprised of only one metal type thus called isopolyoxometalates, or a mixture with other elements (mainly p-block, heteroatoms) thus heteropolyoxometalates. This distinction serves as a valid basis for categorizing POM species. The incorporation of heteroatoms and partial substituents of other metal elements means that the atomic versatility of POM structures is broad, with highly variable compositions and atom numbers ranging from tens to thousands.[2] POMs represent a remarkable class of molecules due to their structural complexity, forming from simple metal salt solutions, affording a rich variety of structural and chemical properties which may be investigated. The composition and structural versatility is reflected in the applications developed around POMs, including in catalysts, electronic devices and materials, utilizing redox, spectroscopic, photovoltaic, and magnetic properties.[3]

One subgroup of POMs is that of giant 'nanosized' polyoxomolybdate clusters, which contain over a hundred molybdenum atoms and have size dimensions similar to proteins, bridging the gap between 'traditional' molecular entities (< 2 nm) and less precisely-defined polymeric entities. Such giant clusters have unique properties and can also be further incorporated into even larger assemblies or high-dimensional materials. During the past two decades there has been much growth in this area since 1996 when Müller et al. determined the first crystal structure of the giant Molybdenum Blue (MB) wheel $\{Mo_{154}\}$.[4] The crystals of the MB wheel were produced from solutions of molybdenum blue which readily develops upon reduction of acidified aqueous molybdate solutions. The identity of the highly soluble species presenting in these molybdenum blue solutions had remained a "mystery" for more than 200 years, exacerbated by difficulties in isolating single crystals suitable for X-ray structure determination. Müller and co-workers finally identified the

Corresponding Author: Leroy Cronin
Address: School of Chemistry, University of Glasgow, Glasgow, G12 8QQ, UK
Tel: +44 7773 321480
E-mail: lee.cronin@glasgow.ac.uk
Keywords: Polyoxometalates, self-assembly, mechanism, autocatalysis, information, molybdenum oxide, molecular replication, templates

conditions necessary to grow crystalline samples of $\{Mo_{154}\}$, mixed-valent wheel-shaped $Mo^{V/VI}$ oxide clusters comprising 154 Mo centers.[5] Later this was extended to the discovery of ball-shaped $\{Mo^{102}\}$,[6] Keplerate-type $\{Mo_{132}\}$,[7] wheel-shaped $\{Mo_{176}\}$,[8] capped wheel $\{Mo_{248}\}$[9] and lemon-shaped $\{Mo_{368}\}$.[10] see Fig. 1 to appreciate the combinatorial nature of these compounds. All these structures have the important transferable pentagonal $\{(Mo)Mo_5\}$ groups in common. Most of them are blue colored as the electrons from reduction are delocalized over the structure, in the central belt spanning the ring, displaying an absorption peak in the long wavelength range (around 750 nm) in the UV-Vis electronic spectra. The Keplerate-type $\{Mo_{132}\}$ is also very highly colored but is an intense brown color and has an absorption peak in the short wavelength range (around 450 nm) in UV-Vis electronic spectra. This is because the electrons are localized in reduced and isolated $\{Mo^{V}\}_2$ Mo–Mo bonds.

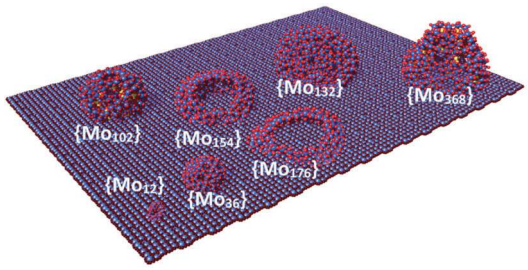

Fig. 1 Combinatorial space of molybdenum oxide clusters. A range of molecules from ones with 12 metal atoms to one with 368 are known. The combinatorial space from which they must be formed is vast. $[PMo_{12}O_{40}]^{3-}$, $\{PMo_{12}\}$; $[Mo_{36}O_{112}(H_2O)_{16}]^{8-}$, $\{Mo_{36}\}$; $[Mo_{102}O_{282}(H_2O)_{78}(CH_3CO_2)_{12}]^{6-}$, $\{Mo_{102}\}$; $[Mo_{132}O_{372}(H_2O)_{72}(CH_3CO_2)_{30}]^{42-}$,$\{Mo_{132}\}$; $[Mo_{154}O_{462}H_{14}(H_2O)_{70}]^{14-}$, $\{Mo_{154}\}$; $[Mo_{176}O_{528}H_{16}(H_2O)_{80}]^{16-}$ $\{Mo_{176}\}$; $[Mo_{368}O_{1032}H_{16}(H_2O)_{240}(SO_4)_{48}]^{48-}$, $\{Mo_{368}\}$.[4–10]

2. Self-Replication

Biological self-replication is driven by complex machinery requiring large amounts of sequence information[11] too complex to have formed spontaneously.[12–14] One route for the emergence of self-replicators is via autocatalytic sets,[15–17] which are collections of units that act cooperatively to replicate. Experimentally autocatalytic sets have been based on RNA, or peptides, and require sequence information.[18] Similarly, the design of directed molecular networks gives insights into how complex self-organised systems build themselves,[19] but these systems are too complex to form randomly. Showing an example outside of biology, would give insights into how the universal 'life-like' chemistry can be. The first suggestion that molybdenum blue chemical systems are governed by a cooperative network of fast reactions was provided by our initial discovery of an intermediate structure in which a central $\{Mo_{36}\}$ cluster appears to template the assembly of the surrounding $\{Mo_{150}\}$ wheel. As a result, it was hypothesised that the formation of such complex gigantic inorganic clusters was only possible due to the utilisation of a number of common building blocks ("Mo_1", "Mo_2" and "Mo_6") able to form embedded autocatalytic sets, see Fig. 2. This is because in general the formation mechanism of large clusters, via the polymerisation of molybdenum oxide, cannot explain why only very specific products are formed, using a building block library which could in principle form thousands of structures of comparable stability. Overcoming thermodynamic and geometry-imposed limitations requires the transfer of key chemical information during the formation cycle, leading to full conversion and finally production of very specific giant molecules. For example, a solution of sodium molybdate at pH 1.7 always produces a cluster containing 36 molybdenum atoms $\{Mo_{36}\}$ in the absence of any added ligands or reducing agents, despite a combinatorial explosion of possibilities. When a reducing agent is used it is possible to produce a family of reduced clusters, and here the nuclearity increases up to a maximum of 368. Even with a reducing agent, less than ten specific classes of large reduced molybdate clusters are known, see Fig. 1, despite an incalculable number of possibilities, while the reactions that form the clusters are fast. Here I explain why the evidence suggests that this system might provide the first concrete example of a self-reproducing autocatalytic set. Such a set requires precise key chemical information for its operation, to demonstrate the first information-rich autocatalytic set observed outside of biology. This is because all prior artificial systems require human-led design of the experiments and the molecular templates.

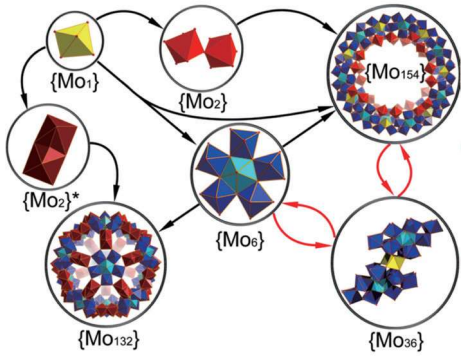

Fig. 2 Hypothetical embedded autocatalytic set which funnels mass from small $\{Mo_1\}$ (yellow polyhedra) monomers into corner-shared (light red), edge-shared (dark red) dimers $\{Mo_2\}$, $\{Mo_6\}$ (blue/cyan polyhedra) building blocks, $\{Mo_{36}\}$ templates and $\{Mo_{132}\}$ Keplerate ball and $\{Mo_{154}\}$ molybdenum blue wheel. The autocatalytic sets enable the members of the set to be produced exponentially faster than competing products.

3. Kinetic Investigations

To investigate the kinetics of the formation of the species the reactions were monitored using stopped-flow with a UV-vis based detection system, see Fig. 3. Here, the contents of syringes containing the reagents for cluster assembly are injected into an observation cell, and the reaction monitored. By setting up the flow system so that it mixed freshly prepared solutions of sodium molybdate and aqueous HCl in equal volumes, it was possible to monitor the absorbance corresponding to the formation of the $\{Mo_{36}\}$ cluster at 350 nm as a function of time. The increase of the concentration $\{Mo_{36}\}$ revealed a sigmoidal relationship which is indicative of an autocatalytic process, see Fig. 3.[20]

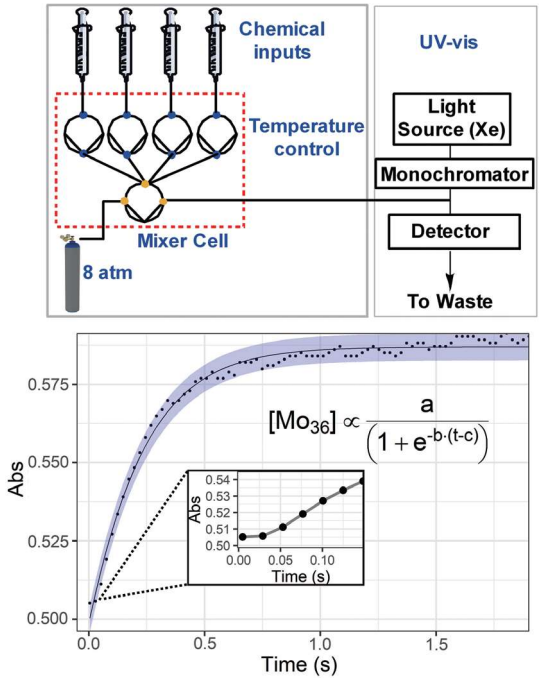

Fig. 3 Top: Experimental set-up and spectroscopic data for $\{Mo_{36}\}$ showing a schematic of the stopped-flow spectrophotometer. The pumps are shown as circles connected to the valves. Bottom: Absorption vs. time profile of $\{Mo_{36}\}$ in water.

It can be hypothesized that the autocatalysis of $\{Mo_{36}\}$ occurs via a molecular recognition process whereby the structure of one cluster acts as coordinate to other fragments allowing the new structure to be formed via hydrogen-bonded and electrostatic interactions. Our studies showed inhibition of the formation of $\{Mo_{36}\}$ when oxalic and trimesic acid were used. In this case the carboxylic acids, which are capable of binding to the constituents of the autocatalytic set in an unproductive manner, decrease the overall rate of the reaction. An alternative way to interrupt the molecular recognition within the autocatalytic set is to prevent the formation or promote the destruction of the species responsible for the formation of the $\{Mo_{36}\}$ cluster. These observations demonstrate the dependence on molecular recognition in driving the rates observed initially during the formation of the $\{Mo_{36}\}$ cluster.

4. Autocatalytic Sets

A key feature of self-replicating and autocatalytic sets is that during the initial stages of the reaction, the process occurs primarily via an uncatalyzed pathway. However, once the product in solution reaches a critical concentration, then the autocatalytic cycle begins to operate. Therefore, the presence of pre-synthesized $\{Mo_{36}\}$, at the beginning of the reaction, (t = 0), should result in no kinetic lag / induction period in the rate profile for the reaction, and an increase of the initial rate and by introducing the $\{Mo_{36}\}$ and we indeed showed that this effect was present. To explore the mechanism a phenomenological model was developed to probe the process of assembly.[20] This was done by making minimal assumptions about the underlying kinetic rate constants, derived from the experimental characterization. To do this we modelled reactions between the monomers and intermediates as reversible reactions and we only considered the structure and the nuclearity of the molecules, see Fig. 4.

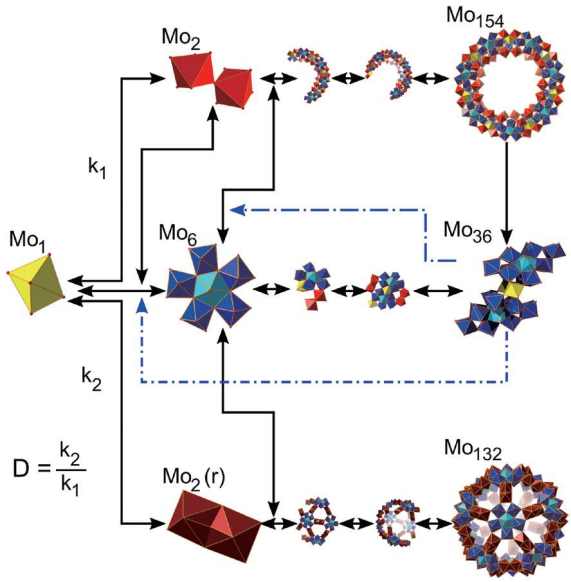

Fig. 4 Schematic representation of the stochastic kinetic model. The model exhibits critical transitions to the formation of the giant nanostructure $\{Mo_{154}\}$ and $\{Mo_{132}\}$.

In the model structures and intermediates were formed as the products of bimolecular reactions between building blocks and other intermediates. To run the model we assumed that all molecules (excluding $\{Mo_1\}$) can degrade into their component parts. The system was initialized the system with

10^6 Mo_1 units and monomers could combine to form different Mo_2 species, the corner bonded dimer and the reduced edge bonded dimer. These two different dimers played different roles in the assembly dynamics, namely the corner bonded dimers can participate in future aggregation to form $\{Mo_6\}$ and other intermediates, while the edge bonded dimers cannot. The edge-bonded dimers can either degrade or bond with $\{Mo_6\}$ and other edge bonded dimers, but not with other $\{Mo_1\}$ species. The relative rate of formation of these two different dimer species is set by the parameter (D) which is the ratio between the rate constant for the formation of edge-bonded dimers to corner bonded dimers.

The following nano-structures were found to form in the model: $\{Mo_{36}\}$, $\{Mo_{132}\}$ (Ball), $\{Mo_{154}\}$ (Wheel), as well as intermediate combinations of those structures and the effect of templating was included in this model. Here, the templates host intermediate compounds and act to enhance the net rate of bimolecular reactions with those intermediates. The templated reactions are decomposed into three separate steps. The first is a bimolecular reaction between a reactant and the template to form complex, followed by another bimolecular reaction between the bound complex and the other reactant. The product of these two steps was found to be a complex of the template and the reactant, which then can then under-go a unimolecular reaction to dissociate. However this complex could also undergo another bimolecular reaction to form a larger product complex before dissociating.

Owing to the combinatorically large number of possible products we also included the effect of templating by assuming that bimolecular reactions between intermediates bound to a template proceeded an order of magnitude faster than reactions without a template. By including this effect to account for the formation of $\{Mo_{154}\}$ templated by $\{Mo_{36}\}$, and then formation of $\{Mo_6\}$, it is possible to propose a mechanism responsible for the autocatalytic properties for $\{Mo_{36}\}$. This model also allowed us to explore the dynamical consequences of different assumptions surrounding the formation of large nano-structure structures. For example, it was proposed that $\{Mo_{36}\}$ templates the formation $\{Mo_6\}$ building blocks, providing a clear mechanism for the autocatalytic behaviour observed for the $\{Mo_{36}\}$ structure.

5. Assembly Theory and Inorganic Complexity

Molecular complexity was initially developed using classical information theory so that molecules can be compared in terms of their size and symmetry.[21] This means many of the approaches are geometric and need topological or graph theoretical analysis with a range of different algorithms.[21] and it is hard to see which of these are intrinsic and also potentially measurable. In our work we have addressed this problem by devising a theory of molecular complexity that is experimentally verifiable. This is because it is possible to place molecules on a scale of complexity from simple to complex. Some molecules are so complex they require a vast amount of encoded information to produce their structures, this means that their formation is very unlikely and needs a lot of help.

Our approach is based on the molecular assembly number (MA) which is derived from the theory of assembly pathways.[22] Assembly pathways are sequences of joining operations, that start with basic building blocks (in this case bonds) and end with a final product. In these sequences, sub-units generated within the sequence can combine with other basic or compound sub-units later in the sequence, to recursively generate larger structures. Assembly pathways have been formalised mathematically using directed multigraphs (graphs where multiple edges are permitted between two vertices) with objects as vertices and objects as edge labels.[21] An issue is that generating many assembly pathways from a pool of basic units will result in a combinatorial explosion in the diversity of structures. As such the molecular assembly number (MA) captures the effects of this combinatorial explosion and provides an agnostic measure of the likelihood for any molecular structure to be produced more than once. There will normally be multiple assembly pathways to create a given molecule. The MA of an object is the length of the shortest of those pathways, i.e., the smallest number of joining operations requires to construct the object, where objects created in the process can subsequently be reused. It is a simple integer metric to indicate the number of steps required in this idealized case to construct the molecule.

The MA of a molecule represents a best-case construction pathway by accounting for bonding rules but not reactivity information. To help determine how the probability of the spontaneous formation of detectable amounts of any given molecule changes with MA, we developed a computational model for the assembly of molecular graphs as unique steps on a path, where the length of this path this represents the MA of a given molecule. The formation of molecules through the assembly process is then modelled using random walks on weighted trees.[24] Here, the root of the tree corresponds to bonds available, while the nodes correspond to possible combinations of those bonds. Each node in the tree therefore corresponds to molecules which could be synthesized from the available bonds, while outgoing edges represent joining

operations transforming one molecule into another with the addition of more bonds. The shortest number of steps on a path from the base of the tree to the end of the branch corresponds to the MA of that compound. These probabilities do not represent the absolute probability of a molecule ever forming, rather they represent the chance of the molecule forming in the unconstrained, undirected process described here in any detectable abundance.

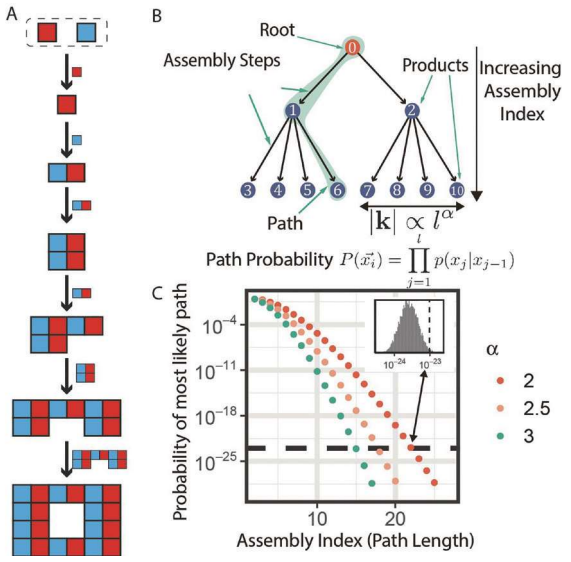

Fig. 5 A) Assembly pathways of an object/ The assembly index of an object is defined as the smallest number of joining operations required to create the object using this model. B) We can model the assembly process as a random walk on weighted trees where the number of outgoing edges (leaves) grows as a function of the depth of the tree, due to the addition of previously made sub-structures. C) The probability of the most likely path through the tree as a function of the path length decreases rapidly.

The MA is determined by searching through partitions of identical substructures, with the algorithm run recursively on those substructures where required. The split-branch MA is calculated by:

$$MA = \begin{cases} \sum_{i=1}^{n} (\mathrm{MA}_i + N_i - 1), & \text{number of bonds} > 1 \\ 1, & \text{number of bonds} = 1 \end{cases}$$

Where the sum is over each duplicated substructure, with representing the number of such duplicates in the structure (the –1 is because the MA is based on the MA of the duplicated substructures plus the number of *additional* copies).

Thermodynamic and kinetic considerations suggest that the relative rates of reactions vary by orders of magnitude, and we implemented this in our model by assigning edge weights (and therefore relative abiotic likelihoods of those reactions) that also span multiple orders of magnitude. The number of possible products for each node in the trees grows as a function of the depth and hence MA of the node. By modelling the rate of growth using a function of the form $|k| \propto l^{\alpha}$, where $|k|$ is the number of possible molecules, l is the depth of the node (l is equal to MA for a given molecule) and α is a parameter that controls how quickly the number of joining operations growths with the depth of the tree. For the combination of any two molecules, the number of possible products formed from their combination grows at least linearly with the size of the compounds, since the bigger compounds have more atoms between which bonds can form. This means the number of ways to produce products in an assembly path explodes as the MA increases since the paths recursively utilize previous steps. To capture this, we evaluated the model with values of α between two and three, where two indicated the most conservative quadratic growth rate, and three representing a limiting case where both factors grow super-linearly. Under these conditions, molecules with a MA of between 15 and 20 would have a chance formation of one molecule in 10^{23}, or one molecule in a mole of substance respectively.

If assembly theory is applied to the clusters, for example the $\{Mo_{154}\}$ or $\{Mo_{132}\}$it can be shown that the assembly number of the ring cluster can be determined by considering the steps in which the building blocks can be added together:

$\{Mo_1\}(+5) \rightarrow \{Mo_6\}(+2) \rightarrow \{Mo_8\}(+3) \rightarrow \{Mo_{11}\}(\times 2) \rightarrow \{Mo_{22}\}(\times 2) \rightarrow \{Mo_{44}\}(\times 2) \rightarrow \{Mo_{88}\}(+44) \rightarrow \{Mo_{132}\}(+22) \rightarrow \{Mo_{154}\}$

MA $\{Mo_{154}\} = 18$; MA $\{Mo_{132}\} = 16$

The hypothesis is that the clusters can be templated by the $\{Mo_{36}\}$ cluster which can be built as follows:

$\{Mo_1\} \rightarrow (+1)\{Mo_2\} \rightarrow (\times 2)\{Mo_4\} \rightarrow (\times 2)\{Mo_8\} \rightarrow (\times 4)\{Mo_{32}\} \rightarrow (+2)\{Mo_{36}\}$ MA $\{Mo_{36}\} = 11$

Following this idea, it seems probable that the $\{Mo_{36}\}$ cluster was produced catalytically using the $\{Mo_{12}\}$ Keggin ion:

$\{Mo_1\}(+2) \rightarrow \{Mo_3\}(\times 4) \rightarrow \{Mo_{12}\}$; MA $\{Mo_{12}\} = 6$

Therefore, the MA driven pathway should proceed

$\{Mo_{12}\} \rightarrow \{Mo_{36}\} \rightarrow \{Mo_{132}\} \rightarrow \{Mo_{154}\}$

We additionally found that the kinetics of formation of the oldest known metal-oxo cluster, the Keggin ion, gave a

sigmoidal trend indicating autocatalysis. Given the ability of the $\{Mo_{36}\}$ to catalyse its own formation, as well as cross-catalytically template the $\{Mo_{154}\}$ molybdenum blue, it was hypothesised if the $\{PMo_{12}\}$ Keggin could also be used to template a new type of Mo-blue. By adding the $\{PMo_{12}\}$ to a reduced acidified solution of $Ce_2O_3{\cdot}7MoO_3{\cdot}6H_2O$ we were able to quickly isolate and crystallize a ring with 124 Mo atoms. The ring was crystallized complete with the $\{PMo_{12}\}$ Keggin template and can be formulated as: $(C_6H_{14}N_2O_4S_2)_4K[H_{16}Mo^{VI}_{100}Mo^{V}_{24}Ce_4O_{376}(H_2O)_{56}(PMo^{VI}_{10}Mo^{V}_{2}O_{40})(C_6H_{12}N_2O_4S_2)_4]{\cdot}200H_2O$ $\{PMo_{12}\} \subset \{Mo_{124}\}$, molybdenum blue wheel, see Fig. 6. Single-crystal X-ray structural analysis reveals that it crystalized in the space group *C*2/*m* and features a nanoring $\{Mo_{124}Ce_4\}$, composed of 12 $\{Mo_8\}$ units, 8 $\{Mo_2\}$ units, 12 $\{Mo_1\}$ units, 4 $\{Ce(H_2O)_5\}$ units and 4 cysteine molecules, with a $\{PMo_{12}\}$ Keggin cluster trapped in the centre. The four Ce^{3+} ions are distributed symmetrically on the two ends of both the upper and lower rims of the $\{Mo_{124}Ce_4\}$ cluster, such that the C_2 symmetric ring has an oval-shaped opening with outer and inner ring diameter of about 29 and 19 Å, respectively. The $\{PMo_{12}\}$ Keggin cluster resides in the middle of the ring on a C_2 axis, and is anchored in place by a number of N–H···O hydrogen-bonds formed with the 4 coordinated cysteine ligands grafted onto the inner ring of $\{Mo_{124}Ce_4\}$.

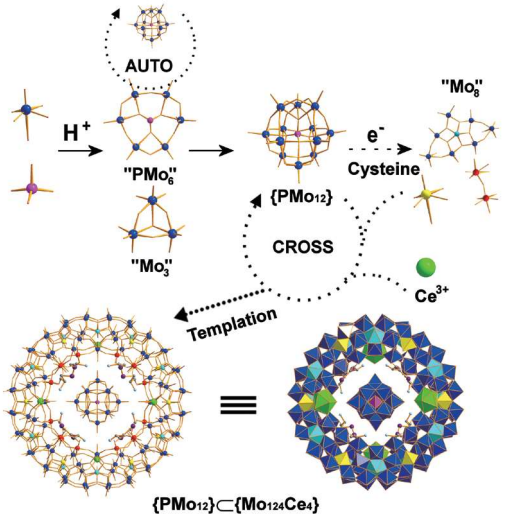

Fig. 6 Autocatalytic and cross-catalytic cycles in the synthesis of $\{Mo_{124}\}$ Wheel. Representation of the minimal autocatalytic set which induces the formation of the Keggin templated $\{Mo_{124}\}$ Wheel.

6. Conclusion

The work described here shows that the formation of an autocatalytic set, which embeds molecular template transfer processes, can form with a simple inorganic system with no explicit template information. We describe how the autocatalytic formation of the $\{Mo_{154}\}$ rings exhibit a critical transition in response to the reduction potential of the solution, due to the coupling between the molecular autocatalyst $\{Mo_{36}\}$ and the formation of $\{Mo_{154}\}$. We hypothesize that the formation of molybdenum nano-structures represents a unique class of self-organized criticality.[22] By analyzing the structures using assembly theory we gain insight into the constraints required to produce the clusters and find that all the clusters can be generated from the simple $\{Mo_{12}\}$ 'seed' template. This is important since it shows how self-assembly of systems undergoing fast kinetics can effectively start to act on each other in a selection process. This is important since all previous autocatalytic sets known are derived from known biology but this study shows how autocatalytic sets, based on simple inorganic salts, can spontaneously emerge which are capable of collective self-reproduction outside of biology.[23]

Acknowledgment

I would like to thank the UK EPSRC, EU ERC, and the University of Glasgow for funding and support doing this work.

References

1 M. T. Pope, A Müller, A. Angew. Chem. Int. Ed. Engl. **1991**, 30, 34–48.

2 a) D.-L. Long, E. Burkholder, L. Cronin, Chem. Soc. Rev. **2007**, 36, 105–121. b) D. -L. Long, R. Tsunashima, L. Cronin, L. Angew. Chem. Int. Ed. **2010**, 49, 1736–1758.

3 a) C. L. Hill, Chem. Rev. **1998**, 98, 1–2. b) E. Coronado, C. Gimenez-Saiz, C. J. Gomez-Garcia, Coord. Chem. Rev. **2005**, 249, 1776–1796. c) H. N. Miras, J. Yan, D.-L. Long, L. Cronin, Chem. Soc. Rev. **2012**, 41, 7403–7430. d) D.-L. Long, L. Cronin, Dalton Trans. **2012**, 41, 9815–9816. e) H. N. Miras, D.-L. Long, L. Cronin, Adv. Inorg. Chem. **2017**, 69, 1–28.

4 A. Müller, J. Meyer, E. Krickemeyer, E. Diemann, Angew. Chem. Int. Ed. Engl. **1996**, 35, 1206-1208.

5 A. Müller, E. Krickemeyer, H. Bogge, M. Schmidtmann, F. Peters, C. Menke, J. Meyer, Angew. Chem. Int. Ed. Engl. **1997**, 36, 484–486.

6 A. Müller, S. Q. N. Shah, H. Bogge, M. Schmidtmann, P. Kogerler, B. Hauptfleisch, S. Leiding, K. Wittler, Angew. Chem. Int. Ed. **2000**, 39, 1614–1616.

7 A. Müller, E. Krickemeyer, H. Bogge, M. Schmidtmann, F. Peters, Angew. Chem. Int. Ed. **1998**, 37, 3360–3363.

8 a) A. Müller, E. Krickemeyer, H. Bogge, M. Schmidtmann, C. Beugholt, P. Kogerler, C. Z. Lu, Angew. Chem. Int. Ed. **1998**, 37, 1220–1223. b) C. C. Jiang, Y. G. Wei, Q. Liu, S. W. Zhang, M. C. Shao, Y. Q. Tang, Chem. Commun. **1998**, 1937–1938. c) A. Müller, M. Koop, H. Bogge, M. Schmidtmann, C. Beugholt, C.

Chem. Commun. **1998**, 1501–1502.
9 A. Müller, S. Q. N. Shah, H. Bogge, M. Schmidtmann, Nature **1999**, 397, 48–50.
10 A. Müller, E. Beckmann, H. Bogge, M. Schmidtmann, A. Dress, Angew. Chem. Int. Ed. **2002**, 41, 1162–1167.
11 P. Nghe, W. Hordijk, S. A. Kauffman, S. I. Walker, F. J. Schmidt, H. Kemble, J. A. M. Yeates, N. Lehman, Mol. Biosyst. **2015**, 11, 3206–3217.
12 T. Tjivikua, P. Ballester, J. Rebek, J. Am. Chem. Soc. **1990**, 112, 1249–1250.
13 D. Sievers, G. von Kiedrowski, Nature **1994**, 369, 221–224.
14 D. H. Lee, J. R. Granja, J. A. Martinez, K. Severin, M. R. Ghadiri, Nature **1996**, 382, 525–528.
15 S. A. Kauffman, J. Theor. Biol. **1986**, 119, 1–24.
16 D. Segre, D. Ben-Eli, D. Lancet, Proc. Natl. Acad. Sci. USA **2000**, 97, 4112–4117.
17 W. Hordijk, M. Steel, J. Syst. Chem. **2013**, 4, 3.
18 T. A. Lincoln, G. F. Joyce, Science **2009**, 323, 1229–1232.
19 G. Ashkenasy, R. Jagasia, M. Yadav, M. R. Ghadiri, Proc. Natl. Acad. Sci. USA **2004**, 101, 10872–10877.
20 H. N. Miras, C. Mathis, W. Xuan, D.-L. Long, R. Pow, L. Cronin, Proc. Natl. Acad. Sci. USA **2020**, 117, 10699–10705.
21 S. M. Marshall, C. Mathis, E. Carrick, G. Keenan, G. J. T. Cooper, H. Graham, M. Craven, P. S. Gromski, D. G. Moore, S. I. Walker, L. Cronin, Nat. Commun. **2021**, 12, 3033.
22 P. Bak, C. Tang, K. Wiesenfeld, Phys. Rev. A **1988**, 38, 364–374.
23 A. G. Cairns-Smith, J. Theor. Biol. **1966**, 10, 53–88.

Profile

Leroy Cronin

Leroy (Lee) Cronin managed to somehow convince the queen of England to allow him to become the Regius Professor of Chemistry in Glasgow (he joined Glasgow as a lecturer and climbed up to this ‘chair’). Since the age of 9 Lee has wanted to explore science using electronics to control matter but was surprised to make it to university as he was deemed to be of sub normal intelligence when he was 12. His research spans many disciplines and has four main aims: the construction of an artificial life form; the digitization of chemistry; the use of artificial intelligence in chemistry including the construction of ‘wet’ chemical computers; the exploration of complexity and information in chemistry. His group is organised and assembled transparently around ideas, avoids hierarchy, and aims to mentor researchers using a problem-based approach. Nothing is impossible until it is tried.